

# Bethe binary-encounter peaks in the double-differential cross sections for high-energy electron-impact ionization of H<sub>2</sub> and He

S. Chatterjee,<sup>1,\*</sup> A. N. Agnihotri,<sup>1</sup> C. R. Stia,<sup>2</sup> O. A. Fojón,<sup>2</sup> R. D. Rivarola,<sup>2</sup> and L. C. Tribedi<sup>1,†</sup>

<sup>1</sup>Tata Institute of Fundamental Research, Homi Bhabha Road, Colaba, Mumbai 400 005, India

<sup>2</sup>Instituto de Física Rosario (CONICET-UNR) and Facultad de Ciencias Exactas, Ingeniería y Agrimensura, Universidad Nacional de Rosario, Av. Pellegrini 250, 2000 Rosario, Argentina

(Received 11 January 2010; published 30 November 2010)

We study the Bethe binary-encounter (BE) region in the ejected-electron double-differential emission spectrum of H<sub>2</sub> and He targets in collisions with 8-keV electrons. We compare the absolute cross sections for these isoelectronic systems at high emission energies. The experimental data are analyzed in terms of a state-of-the-art theoretical model based on a two-effective-center approximation. In the case of the H<sub>2</sub> molecule the binary peak in the double-differential cross sections (DDCS) is enhanced due to the two-center Young-type interference. The observed undulation in the DDCS ratio is explained in terms of the combined contributions of the Compton profile mismatch and the interference effect. The influence of the interference effect is thus observed for higher-energy electrons compared to most of the earlier studies which focused on low-energy electrons produced in soft collisions.

DOI: [10.1103/PhysRevA.82.052709](https://doi.org/10.1103/PhysRevA.82.052709)

PACS number(s): 34.50.Gb, 34.80.Gs, 03.75.-b

## I. INTRODUCTION

The study of ionization of atoms and molecules by ion or electron beams or photons has been a topic of interest in the field of atomic collision physics for many decades. The crucial information regarding the ionization process and hence about the basic collision mechanisms can be obtained by detecting the electron spectrum in such collision processes. For heavy-ion beams the distinct ionization processes appear in the double-differential cross section (DDCS) spectrum of ejected electrons. The main processes are the soft collisions (SC), the two-center electron emission (TCEE), the electron capture to the continuum (ECC), and the binary encounter (BE) [1]. For the TCEE, the ejected electron in the final channel is influenced by the strong Coulomb potential of the receding highly charged projectile and may show a focusing effect in the forward direction [2–8]. Such a two-center effect is less relevant when electrons are used as projectiles, since they are singly charged particles [9]. However, SC and BE are dominant features besides the elastic-scattering peak in electron collisions with atoms. Many experimental and theoretical investigations on the BE process in heavy-ion collisions have been reported in the past [4,10,11]. In the case of electron-impact ionization an elaborate measurement on the BE process is scarce. We present here a detailed study of the BE process for fast-electron collisions with H<sub>2</sub> and He.

The ionization of homonuclear diatomic molecules may also carry rich information about the wave nature of the ionized electron. Such a wave nature is manifested via the oscillations in the electron spectrum due to Young-type interference [12,13] that occurs as a consequence of coherent electron emission from the proximities of the nuclei of the molecular target. This effect was first observed only recently in the electron spectra resulting from the ionization of molecular

hydrogen by heavy-ion impact [14–20] and in photoionization studies involving H<sub>2</sub>, N<sub>2</sub>, and H<sub>2</sub><sup>+</sup> targets [21–28]. The interference mechanism in electron scattering from molecular H<sub>2</sub> was invoked as early as 1977. For example, the oscillation in the cross section ratios (H<sub>2</sub> to 2H) in the case of elastic scattering of projectile electrons was found both theoretically and experimentally [29,30]. In electron-impact ionization studies, the presence of oscillations due to coherent emission was predicted [31] and then experimentally observed in DDCSs [32] and later on in the angular distribution of electron emission [33–35] for H<sub>2</sub> in coplanar kinematics by investigating the relative change of binary and recoil peak intensities caused by partial constructive or destructive interferences. In triple-differential cross section (TDCS) studies, the single-center He target was also used as a reference to compare the fluctuation of intensity due to interference effects in the corresponding H<sub>2</sub> spectrum [33,34]. Recently, Young-type interference patterns were reported in the double-electron capture process from molecular hydrogen [36].

In the present work, we have investigated the behavior of the Bethe binary encounter peak appearing in the energy distribution of electron DDCSs of H<sub>2</sub> and He in collisions with 8-keV electrons. Young-type interferences are analyzed in the BE region for H<sub>2</sub> by comparing with the corresponding results for He. The role of BE electrons in the low ejection energies is studied at different forward angles. A detailed comparison is made for energy distributions of DDCSs between the cases of H<sub>2</sub> and He targets at low ejection energies and it is demonstrated that the presence of varying strengths of partial constructive interferences modify the H<sub>2</sub> cross sections.

## II. EXPERIMENTAL DETAILS

The measurements were carried out for an 8-keV ( $v_p \sim 24$  a.u.) electron beam colliding with H<sub>2</sub> and He gaseous targets. The electron beam was generated from a commercial electron gun. In addition to the built-in focusing element in the electron gun, we mounted another set of Einzel lens, deflector, and collimator assembly at the entrance of the chamber to

\*Present address: Indian Institute of Technology, Bhubaneswar, Orissa, 751013, India

†lokesh@tifr.res.in

focus the beam at the center of the chamber. The electrons emitted from the target were detected using an electron spectrometer equipped with a hemispherical electrostatic energy analyzer and a channel electron multiplier (CEM). Care was taken regarding the spectrometer performance, stray fields, background electrons, and projectile beam profile. The energy resolution of the spectrometer was about 6% of the electron energy which was limited by the entrance and exit apertures. Experiments were done by flooding the chamber, keeping the target gas pressure in the range of 0.15–0.25 mTorr. The front and exit apertures of the spectrometer were biased to small voltages of +6 V in order to help the low-energy electrons be detected. Background pressure was kept at  $1 \times 10^{-7}$  Torr. We normalized the measured data of H<sub>2</sub> and He with respect to known absolute DDCSs obtained in our earlier measurements [37]. The relative systematic uncertainty stemming from the measuring system is about  $\pm 16\%$ – $18\%$ . Further details of the experimental setup are described in Refs. [37,38]. The electron DDCS data were corrected for the efficiency of the CEM as described in Ref. [38].

### III. BETHE BINARY-ENCOUNTER PEAK AND INTERFERENCE EFFECT

The electron-impact BE process is quite different from that for heavy ions because of their large difference of masses. In the case of binary encounter for heavy-ion beams colliding on atoms the electrons suffer Rutherford backscattering from a huge mass when viewed from a frame fixed on the projectile [4,10,11], assuming that all the momentum is transferred to the emitted electron (Bethe condition). In the laboratory system, the energetic position of the corresponding peak appearing in differential cross sections, according to energy and momentum conservation rules, is given by

$$E_{\text{BE}} = 4t \cos^2 \theta_e - 2I, \quad (1)$$

where the cusp electron energy is given by  $t = (M_e/M_p)E_p$ , where  $M_e$  and  $M_p$  are the electron mass and the projectile mass, respectively. Here  $\theta_e$  is the electron ejection angle and  $I$  denotes the target ionization energy. In the case of electron-atom collisions, the binary-encounter peak position

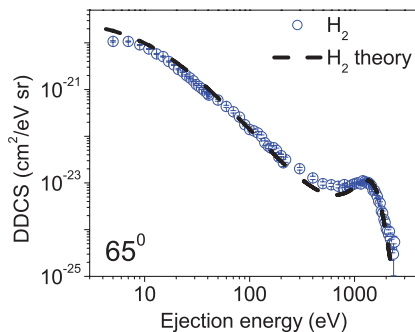


FIG. 1. (Color online) DDCS spectrum of electrons ejected in 8-keV  $e^- + \text{H}_2$  collisions for  $65^\circ$  ejection angle. The dashed line represents theoretical predictions using a two-effective-center approximation.

in the electron DDCS spectrum is given by,

$$E_{\text{BE}} = E_p \cos^2 \theta_e - I. \quad 0 \leq \theta_e \leq 90^\circ. \quad (2)$$

In both the Eqs. (1) and (2),  $E_p$  represents the projectile kinetic energy.

Measured DDCSs for electron emission from H<sub>2</sub> are presented in Fig. 1 as a function of the ejected electron energy at fixed ejection angle  $\theta_e = 65^\circ$ . According to Eq. (2), the BE peak in DDCS spectrum is shown (see Fig. 1) to appear at an ejection energy of  $\sim 1400$  eV for emission angle  $65^\circ$  ejection angle is analyzed. The experimental data are in general in good agreement with the theoretical prediction, also included in Fig. 1. Calculations were performed using the two-effective-center (TEC) approximation [39], which will be used for all H<sub>2</sub> cases considered. Briefly, the TEC approximation is based on the localized nature of the initial electronic density around the molecular nuclei. The emission of one of the target electrons is considered as produced preferably from the vicinity of either molecular center, whereas the other electron screens completely the nucleus corresponding to the region from which ionization is not produced. The final continuum wave function of the ejected electron is chosen in the TEC model as an effective one-center Coulomb wave function taking into account the interaction of the emitted electron with one or the other molecular nucleus [39]. Also, a Heitler-London-type wave function [40] was used to describe the initial bound molecular state. With all these assumptions and following Ref. [31], the DDCS of ionization of H<sub>2</sub> molecules is obtained from the expression [9,32,37]

$$\frac{d^2\sigma_{\text{H}_2}}{d\Omega_e dE_e} \cong \int d\Omega_s \left[ 1 + \frac{\sin(\chi\rho)}{\chi\rho} \right] \frac{d^3\sigma_{2\text{H}_{\text{eff}}}}{d\Omega_s d\Omega_e dE_e}, \quad (3)$$

where  $\Omega_s$  and  $\Omega_e$  are the solid angles subtended by the scattered projectile and the ejected electron, respectively,  $E_e$  is the final energy of the ionized electron,  $\chi = |\vec{k}_e - \vec{K}|$  with  $\vec{k}_e$  being the momentum of the ejected electron and  $\vec{K}$  the momentum transfer, and  $\rho$  is the equilibrium internuclear distance. The TDCS  $d^3\sigma_{2\text{H}_{\text{eff}}}/d\Omega_s d\Omega_e dE_e$  refers to two effective H atoms ( $\text{H}_{\text{eff}}$ ) located at the position of each molecular nucleus. It is noted that the interference factor  $1 + \sin(\chi\rho)/\chi\rho$  due to coherent emission from both molecular centers appears explicitly in Eq. (3). Indeed, for BE ejected electrons  $\vec{k}_e = \vec{K}$  and thus the term  $1 + \sin(\chi\rho)/\chi\rho \simeq 2$  in Eq. (3) contributes as constructive interference.

In Figs. 2(a) and 2(b), TEC cross sections for H<sub>2</sub> (dashed lines) are compared with the ones corresponding to two  $\text{H}_{\text{eff}}$  atoms (dotted lines). The latter one-center DDCSs were obtained from Eq. (3) by neglecting the damping oscillatory interference term. In Fig. 2(a) the ejection angle is  $\theta_e = 55^\circ$ , whereas in Fig. 2(b),  $\theta_e = 65^\circ$ . It is observed that molecular cross sections are larger than the atomic ones in the BE peak, supporting the presence of partial constructive interference in this region. Even considering that Eq. (3) is strictly valid when comparing the DDCS for the hydrogen molecule and the one for effective hydrogen atomic targets, the presence of Young-type interference effects could also be put in evidence if helium atomic targets were used to obtain the DDCS H<sub>2</sub>/He ratios as shown below. In early works by Milne-Brownlie *et al.* [33] and Staicu Casagrande *et al.* [34], it was shown

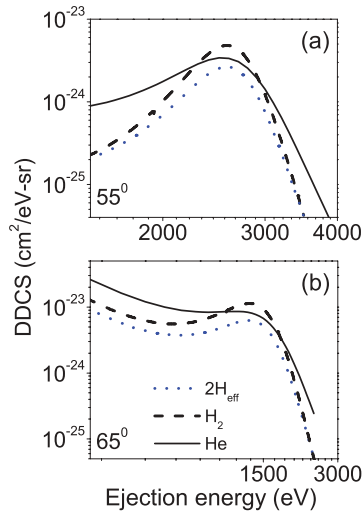


FIG. 2. (Color online) Theoretical cross sections for molecular hydrogen (dashed line), He (solid lines), and twice  $H_{\text{eff}}$  (dotted line) are plotted for  $55^\circ$  (a) and  $65^\circ$  (b).

that the TDCS ratios for  $H_2$  and He targets are qualitatively well described by the oscillatory factor  $1 + \sin(\chi\rho)/\chi\rho$  of Eq. (3).

In Figs. 2(a) and 2(b), theoretical DDCSs for He atoms are also displayed (solid lines) for comparison. In these calculations, a first-order Born approximation is employed. Within the framework of this model, both the incident and the scattered electrons are described by plane waves, whereas the initial atomic bound state is described by a Löwdin's wave function [41]. The final continuum state for the ionized electron is chosen as a continuum wave function corresponding to the interaction between the emitted electron and the residual target at large asymptotic separations. It has been shown that this first-order model gives a good description of the measured TDCS for ionization of He atoms at an incident-electron energy of around 8 keV [42]. From Fig. 2, it is also found that the calculated molecular cross sections are larger than the corresponding cross sections for He atoms, suggesting the presence of constructive interferences around the BE peak position.

The experimental DDCSs near the BE region for the two isoelectronic systems,  $H_2$  and He, are shown in Fig. 3 for four different angles, namely,  $55^\circ$ ,  $60^\circ$ ,  $70^\circ$ , and  $75^\circ$ , along with the corresponding theoretical results. With increasing angle the agreement between theory and experiment becomes better with respect to the peak position and the overall shape of the cross sections. In fact, theory has better agreement with experimental data for the larger forward angles  $70^\circ$  and  $75^\circ$  compared to  $55^\circ$  and  $60^\circ$ . At the peak positions where the cross sections are large, the statistical uncertainty is about 5–8%. For smaller angles such as  $55^\circ$  and  $60^\circ$ , at some points at lower energies where the cross section falls, the statistical uncertainty is as large as 40%. For  $H_2$  at the particular angle  $55^\circ$  [Fig. 3(e)], a large difference between the theoretical results and the experimental results is observed at lower energies. This behavior is not well understood and must be a matter of further investigation, considering first the influence of more precise descriptions of the molecular continuum wave functions as the electron is ejected in the forward direction.

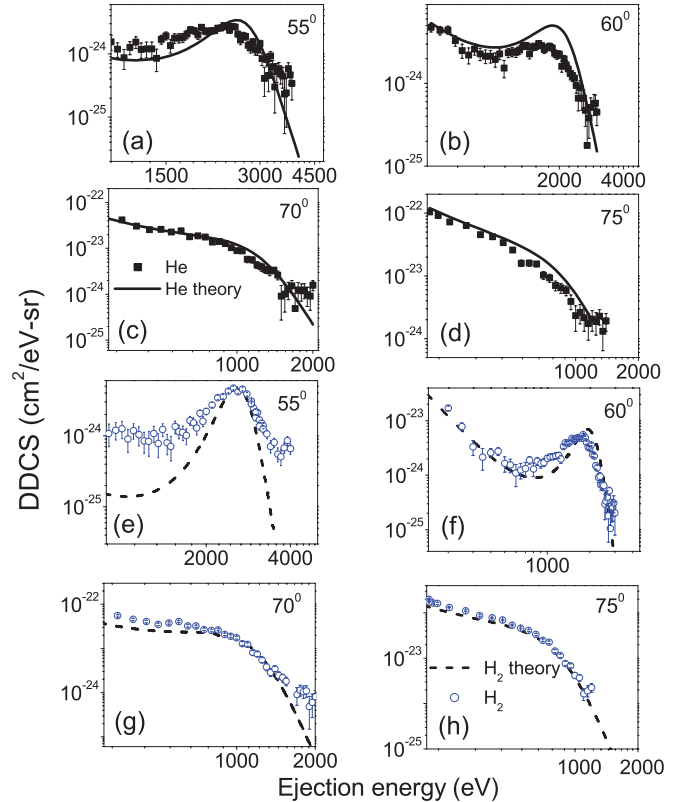


FIG. 3. (Color online) The experimental and theoretical DDCSs for four different angles, namely,  $55^\circ$ ,  $60^\circ$ ,  $70^\circ$ , and  $75^\circ$ , are plotted. Panels (a) to (d) represent cross sections for He, and panels (e) to (h) represent cross sections for  $H_2$ . The lines are the theoretical DDCS values.

For almost all angles, differences between experimental and theoretical DDCSs of  $H_2$  for emission energies larger than the one corresponding to the BE peak could be attributed to elastic scattering which has not been included in the calculations. For instance, the scattered projectile electrons, which lose energy during the collision process may contribute at high ejection energies after the BE peak in the case of forward angles. The contribution of such scattered electrons increases with ejection energy and reaches maximum at the elastic peak [43].

In Fig. 4(a) we display the DDCSs in the energy range of 900–2700 eV for the case of  $\theta_e = 65^\circ$ . The experimental cross section of  $H_2$  at the BE peak clearly exceeds the experimental cross section for He. We observe also the same behavior in the corresponding theoretical DDCSs [see also Fig. 2(a) for  $55^\circ$ ]. For the current study we explore the contribution of interference in the BE region by taking the DDCS ratio

$$R = \frac{d^2\sigma_{H_2}}{d\Omega_e dE_e} \bigg/ \frac{d^2\sigma_{He}}{d\Omega_e dE_e} \quad (4)$$

The experimental ratio of the electron DDCSs for  $H_2$  and He targets for ejection angle  $65^\circ$  is plotted in Fig. 2(b). The experimental ratio exhibits a peaked structure with a maximum value around the position of the BE, which is supported by the theoretical prediction. Such behavior may be originated from the combined contributions of interference effects and the different Compton profiles of the target electrons (of  $H_2$  and He). In order to quantify the presence of interference

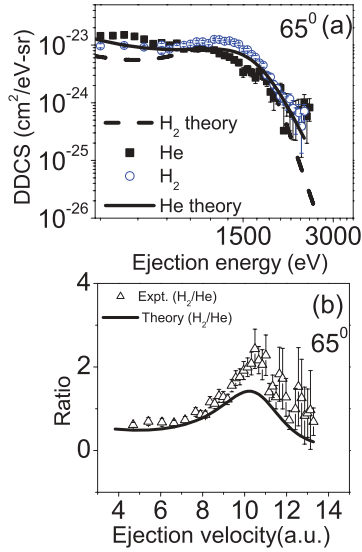


FIG. 4. (Color online) (a) Experimental DDCSs are represented by open circles ( $H_2$ ) and solid squares (He) and theories are represented by a dashed line ( $H_2$ ) and a solid line (He) for 8-keV  $e$  impact. (b) Triangles represent complete experimental ratios of  $H_2/He$ , and complete theoretical ratios are shown as a solid line.

effects in the structure, we compute the DDCS ratio for molecular hydrogen and two  $H_{\text{eff}}$  atoms and compare it with the theoretical one between the  $H_2$  and He targets for two different ejection angles of  $55^\circ$  and  $65^\circ$  [Figs. 5(a) and 5(b), respectively]. The atomic  $2H_{\text{eff}}/He$  ratio is also included in Fig. 5. It is well known that the DDCS is proportional to the corresponding Compton profiles when a plane-wave B1 approximation is used to investigate the reaction [14]. The cross section ratio can then be expressed as the one corresponding to the different Compton profiles of the considered targets. Thus, the behavior of the  $2H_{\text{eff}}/He$  ratio

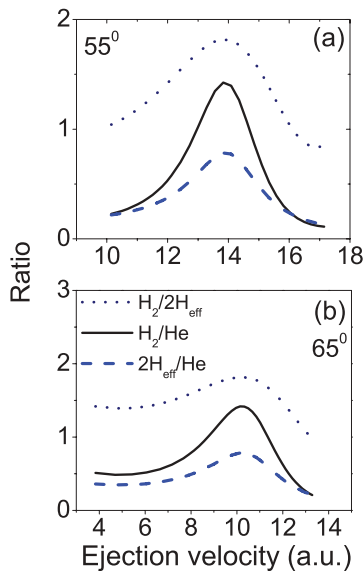


FIG. 5. (Color online) The ratios of theoretical DDCSs for  $H_2/2H_{\text{eff}}$  (dotted lines),  $H_2/He$  (solid lines), and  $2H_{\text{eff}}/He$  (dashed lines) are plotted for two different ejection angles:  $55^\circ$  (a) and  $65^\circ$  (b).

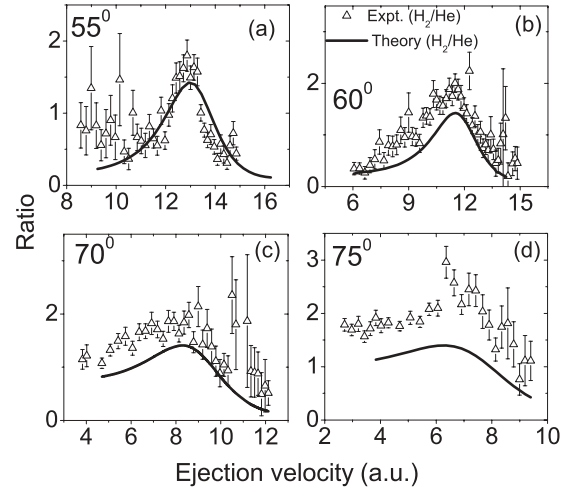


FIG. 6. Ratio spectra for four different ejection angles:  $55^\circ$  (a),  $60^\circ$  (b),  $70^\circ$  (c), and  $75^\circ$  (d). Open triangles, experimental ( $H_2/He$ ); solid lines, theoretical ( $H_2/He$ ). Note that the theoretical ratio of panel (a) is shifted by 0.9 a.u. and of panel (b) by 0.6 a.u. toward lower velocity to compare with the experimental data.

(dashed lines) can be attributed to these different profiles for  $H_{\text{eff}}$  and He atoms. Consequently, a hump can be observed for electron velocities in the corresponding ratio at the binary encounter position. Regarding the  $H_2/2H_{\text{eff}}$  ratio, it shows the contribution of the interference term in Eq. (3). In fact, both  $H_2$  and  $2H_{\text{eff}}$  DDCSs differ in a factor of the order of 2, in qualitative agreement with the value obtained from this interference term as  $\vec{k}_e = \vec{K}$ . As a result of the combination of both Compton profile and interference contributions, a sharper enhancement is found in the  $H_2/He$  ratio (solid lines). While the undulation in the experimental  $H_2/He$  data may primarily be stemming from the mismatch of Compton profiles, we find a significant contribution of constructive interference around the Bethe binary encounter peak for the  $H_2/He$  DDCS ratio.

In Fig. 6 we illustrate the DDCS ratios of  $H_2$  and He for all the four angles considered previously in Fig. 3. It is observed that the experimental results vary within the values 0.5 and 2, represented by the mismatch of the Compton profiles of the targets. They are in good agreement with the theoretical predictions. In some cases we find a sharp enhancement of the  $H_2$  BE peak by constructive interference, behavior that is supported by our previous analysis. In fact, we demonstrate thus the existence of Young-type coherent emission at ejection velocities as high as 8–15 a.u., where the corresponding de Broglie wavelength becomes shorter than in all previous measurements, which were done below 6 a.u.

#### IV. BINARY-ENCOUNTER ELECTRONS IN LOW-EJECTION ENERGY

Figures 7(a) to 7(d) show the measured energy distributions of DDCSs for  $45^\circ$ ,  $75^\circ$ ,  $90^\circ$ , and  $135^\circ$ , respectively, for the same systems described previously. Going through Figs. 7(a) to 7(d) we note relative change in the DDCSs of  $H_2$  [37] and He. For example, Figs. 7(a) and 7(d) show crossovers between the DDCS of  $H_2$  and He at about 20 eV. Since in the case of  $45^\circ$  the binary peak has the least overlap with the

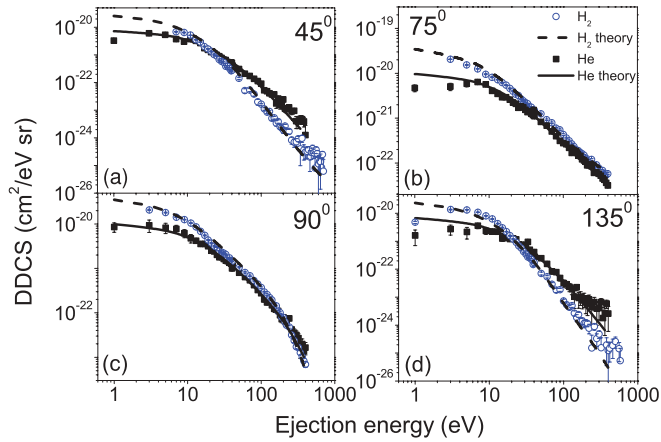


FIG. 7. (Color online) Energy distributions of DDCSs of electrons ejected from  $\text{H}_2$  (open circles) [37] and He (solid squares) in collisions of 8-keV  $e^-$  for ejection angles  $45^\circ$  (a),  $75^\circ$  (b),  $90^\circ$  (c), and  $135^\circ$  (d). The theoretical predictions for  $\text{H}_2$  are shown as dashed lines and for He as solid lines.

one corresponding to low-energy electrons, the low-energy spectrum is dominated by the soft collision mechanism. This will, however, be influenced by the interference process for  $\text{H}_2$  but not for He. Similarly for backward angles the spectrum is only influenced by the soft collision along with the interference for  $\text{H}_2$ . The crossover observed for these two angles can possibly be explained by the interference mechanism present in the case of the  $\text{H}_2$  spectrum. However, for angles closer to  $90^\circ$  [Figs. 7(b) and 7(c)] the spectra for He and  $\text{H}_2$  merge together at high ejection energies. Since the BE peak energy scales as  $\cos^2 \theta_e$  [see Eq. (2)], the peak shifts toward lower ejection energies as  $\theta_e$  increases. Close to  $90^\circ$  the BE electrons merge with low-energy electrons. In sharp contrast to the  $45^\circ$  and  $135^\circ$  cases, in Fig. 7, the DDCSs for  $\text{H}_2$  for  $75^\circ$  and  $90^\circ$  are considerably raised to larger values when compared to the similar results for He in the range of ejection energies contained between 20 and 500 eV. Because we have shown (see earlier in this article) that in the BE region the constructive interference enhances the electron DDCSs for  $\text{H}_2$  compared to those for He, the present large DDCS at the low-energy part of the spectrum could be attributed to a similar process. So the overall shape can be attributed to the presence of low-energy BE electrons and to the associated partial constructive interference in the case of  $\text{H}_2$ , for angles close to  $90^\circ$ .

For all the four angles considered in Fig. 7, below 30-eV ejection energies, the DDCSs for He always fall below those

for molecular  $\text{H}_2$  beyond the experimental uncertainties. The presence of constructive interference in the DDCS for  $\text{H}_2$  may be possible in the low-energy (or soft collision) region ( $k_e \simeq 0$ ), where the momentum transfer from the projectile is very small ( $K \simeq 0$ ), and this may lead to a significant enhancement of the DDCS for  $\text{H}_2$  compared to that of He. However, we note that contributions from autoionization processes for  $\text{H}_2$  below 20 eV [44] and electron correlation effects and detailed screening effects at low ejection energies for both the targets may also contribute to the structures, which are not included in the current theoretical calculations. A similar behavior regarding the role of constructive interference in the BE and SC regions was also observed earlier when we compared the  $\text{H}_2$  results (both experimental and theoretical) with those of corresponding twice  $\text{H}_{\text{eff}}$  [37]. As a matter of fact, the simultaneous promotion of electrons to continuum states through BE and soft collision mechanisms for angles close to  $90^\circ$  reinforces the presence of partial constructive interference and, moreover, this effect is extended to larger values of the energy spectra.

## V. CONCLUSIONS

In conclusion, we have studied binary-encounter electron emission from molecular hydrogen and helium targets in collisions with 8-keV electrons. We have compared the absolute DDCSs of electrons ejected at high energies from the two isoelectronic systems. The DDCS ratio ( $\text{H}_2/\text{He}$ ) shows undulation between 0.5 and 2, which may be stemming from the combined contributions of the Compton profiles of the target electrons and the interference effects. It is demonstrated that the cross section of the BE peak for  $\text{H}_2$  is enhanced by the constructive interference due to coherent emission from the two H centers of the molecule. We investigated the presence of interference effects in the energy spectrum as the BE peak moves toward lower ejection energies with increasing angle. In all cases studied, theoretical predictions reasonably support the experimental analysis.

## ACKNOWLEDGMENTS

We acknowledge the cooperation of S. Kasthurirangan, K. V. Thulasiram, and N. Mhatre during the experiment. C.R.S, O.A.F., and R.D.R. acknowledge financial support from the Agencia Nacional de Promoción Científica y Tecnológica (PICT No. 02040 and PICT No. 01912), and the Consejo Nacional de Investigaciones Científicas y Técnicas de la República Argentina (PIP No. 11220090101026).

- 
- [1] N. Stolterfoht, R. D. Dubois, and R. D. Rivarola, *Electron Emission in Heavy Ion-Atom Collisions*, Springer Series on Atoms and Plasmas, Vol. 20 (Springer-Verlag, Heidelberg, 1997).
- [2] P. D. Fainstein, V. H. Ponce, and R. D. Rivarola, *J. Phys. B* **24**, 3091 (1991).
- [3] N. Stolterfoht, H. Platten, G. Schiwietz, D. Schneider, L. Gulyás, P. D. Fainstein, and A. Salin, *Phys. Rev. A* **52**, 3796 (1995).
- [4] J. O. P. Pedersent, P. Hvelplundt, A. G. Petersent, and P. D. Fainstein, *J. Phys. B* **24**, 4001 (1991).
- [5] S. Suarez, C. Garibotti, W. Meckbach, and G. Bernardi, *Phys. Rev. Lett.* **70**, 418 (1993).
- [6] P. D. Fainstein, L. Gulyás, F. Martín, and A. Salin, *Phys. Rev. A* **53**, 3243 (1996).
- [7] L. C. Tribedi, P. Richards, W. DeHaven, L. Gulyás, M. W. Gealy, and M. E. Rudd, *J. Phys. B* **31**, L369 (1998).
- [8] D. Misra, A. Kelkar, U. Kadhane, A. Kumar, L. C. Tribedi, and P. D. Fainstein, *Phys. Rev. A* **74**, 060701(R) (2006).
- [9] S. Chatterjee, D. Misra, A. H. Kelkar, L. C. Tribedi, C. R. Stia, O. A. Fojón, and R. D. Rivarola, *Phys. Rev. A* **78**, 052701 (2008).

- [10] N. Stolterfoht, D. Schneider, R. Burch, H. Wieman, and J. S. Risley, *Phys. Rev. Lett.* **33**, 59 (1974).
- [11] D. H. Lee, P. Richard, T. J. M. Zouros, J. M. Sanders, J. L. Shnappaugh, and H. Hidmi, *Phys. Rev. A* **41**, 4816 (1990).
- [12] J. A. R. Samson and R. B. Cairns, *J. Opt. Soc. Am.* **55**, 1035 (1965).
- [13] H. D. Cohen and U. Fano, *Phys. Rev.* **150**, 30 (1966).
- [14] N. Stolterfoht *et al.*, *Phys. Rev. Lett.* **87**, 023201 (2001).
- [15] D. Misra, U. Kadhane, Y. P. Singh, L. C. Tribedi, P. D. Fainstein, and P. Richard, *Phys. Rev. Lett.* **92**, 153201 (2004); see also J. A. Tanis, S. Hossain, B. Sulik, and N. Stolterfoht, *ibid.* **95**, 079301 (2005); D. Misra, U. Kadhane, Y. P. Singh, L. C. Tribedi, P. D. Fainstein, and P. Richard, *ibid.* **95**, 079302 (2005).
- [16] S. Hossain, A. S. Alnaser, A. L. Landers, D. J. Pole, H. Knutson, A. Robison, B. Stamper, N. Stolterfoht, and J. A. Tanis, *Nucl. Instrum. Methods Phys. Res. B* **205**, 484 (2003).
- [17] S. Hossain, A. L. Landers, N. Stolterfoht, and J. A. Tanis, *Phys. Rev. A* **72**, 010701(R) (2005).
- [18] D. Misra, A. Kelkar, U. Kadhane, A. Kumar, Y. P. Singh, L. C. Tribedi, and P. D. Fainstein, *Phys. Rev. A* **75**, 052712 (2007).
- [19] D. Misra, Aditya H. Kelkar, S. Chatterjee, and L. C. Tribedi, *Phys. Rev. A* **80**, 062701 (2009).
- [20] S. Chatterjee, D. Misra, A. H. Kelkar, P. D. Fainstein, and L. C. Tribedi, *J. Phys. B* **42**, 125201 (2010).
- [21] D. Rolles *et al.*, *Nature (London)* **437**, 711 (2005).
- [22] X.-J. Liu *et al.*, *J. Phys. B* **39**, 4801 (2006).
- [23] K. Kreidi *et al.*, *Phys. Rev. Lett.* **100**, 133005 (2008).
- [24] D. Akoury *et al.*, *Science* **318**, 949 (2007).
- [25] R. Della Picca, P. D. Fainstein, M. L. Martiarena, N. Sisourat, and A. Dubois, *Phys. Rev. A* **79**, 032702 (2009).
- [26] O. A. Fojón, J. Fernández, A. Palacios, R. D. Rivarola, and F. Martín, *J. Phys. B* **37**, 3035 (2004).
- [27] J. Fernández, O. Fojón, A. Palacios, and F. Martín, *Phys. Rev. Lett.* **98**, 043005 (2007).
- [28] J. Fernández, O. Fojón, and F. Martín, *Phys. Rev. A* **79**, 023420 (2009).
- [29] D. K. Jain and S. P. Khare, *Phys. Lett. A* **63**, 237 (1977).
- [30] A. Jain, A. N. Tripathi, and M. K. Srivastava, *Phys. Rev. A* **20**, 2352 (1979).
- [31] C. R. Stia, O. A. Fojón, Ph. Weck, J. Hanssen, and R. D. Rivarola, *J. Phys. B* **36**, L257 (2003).
- [32] O. Kamalou, J.-Y. Chesnel, D. Martina, F. Frémont, J. Hanssen, C. R. Stia, O. A. Fojón, and R. D. Rivarola, *Phys. Rev. A* **71**, 010702(R) (2005).
- [33] D. S. Milne-Brownlie, M. Foster, J. Gao, B. Lohmann, and D. H. Madison, *Phys. Rev. Lett.* **96**, 233201 (2006).
- [34] E. M. Staicu Casagrande *et al.*, *J. Phys. B* **41**, 025204 (2008).
- [35] O. A. Fojón, C. R. Stia, and R. D. Rivarola, *AIP Conf. Proc.* **811**, 42 (2006).
- [36] D. Misra *et al.*, *Phys. Rev. Lett.* **102**, 153201 (2009).
- [37] S. Chatterjee, S. Kasthurirangan, A. H. Kelkar, C. R. Stia, O. A. Fojón, R. D. Rivarola, and L. C. Tribedi, *J. Phys. B* **42**, 065201 (2009).
- [38] D. Misra, K. V. Thulasiram, W. Fernandes, A. H. Kelkar, U. Kadhane, A. Kumar, Y. Singh, L. Gulyas, and L. C. Tribedi, *Nucl. Instrum. Methods Phys. Res. A* **267**, 157 (2009).
- [39] P. Weck, O. A. Fojón, J. Hanssen, B. Joulakian, and R. D. Rivarola, *Phys. Rev. A* **63**, 042709 (2001).
- [40] S. C. Wang, *Phys. Rev.* **31**, 579 (1928).
- [41] P. O. Löwdin, *Phys. Rev.* **90**, 120 (1953).
- [42] Lahmann-Bennani *et al.*, *J. Phys. B* **16**, 2219 (1983).
- [43] N. Oda, *Radiat. Res.* **64**, 80 (1975).
- [44] J. Y. Chesnel, D. Martina, P. Sobocinski, O. Kamalou, F. Frémont, J. Fernández, and F. Martín, *Phys. Rev. A* **70**, 010701(R) (2004).